Ma, X.X., Xu, Z., Mao, X., Cawood, T., Yan, H., Gao, J., Si, J.L., and Li, H.B., 2023, A tale of an orbicule in the eastern Gangdese belt of southern Tibet: petrographic, geochemical and submagmatic structural perspectives on its formation: GSA Bulletin, https://doi.org/10.1130/B36607.1.

Supplemental Material

Table S1. Zircon LA-ICPMS U-Pb dating results for the orbicule matrix and orbicule core in the Gangdese belt, southern Tibet.

Table S2. Zircon trace elemental results for the orbicule matrix and orbicule cores in the Gangdese belt, southern Tibet.

Table S3. Whole-rock geochemical data for the orbicule matrix and orbicule core in the Gangdese belt, southern Tibet.

Table S4. Zircon Lu-Hf isotopic results for the orbicule matrix and orbicule core in the Gangdese belt, southern Tibet.

Table S5. Whole-rock Sr-Nd data for the orbicule matrix and orbicule cores in the Linzhi region of the eastern Gangdese magmatic belt, Eastern Himalayan Syntaxis.

Table S6. Hornblende electron microprobe analyzed data for the orbicule matrix, orbicule shells and orbicule cores in the Gangdese belt, southern Tibet.

Figure S1. Field photos and photomicrographs of the collected orbicule in the Gangdese belt, southern Tibet.

Figure S2. Representative zircon Cathodoluminescence (CL) images and the spots for the zircon U-Pb and Lu-Hf analyses.

Figure S3. Whole-rock Harker diagrams and trace elemental spider diagrams for the matrix and core of the orbicule.

Supplemental Text. Analytical Methods.

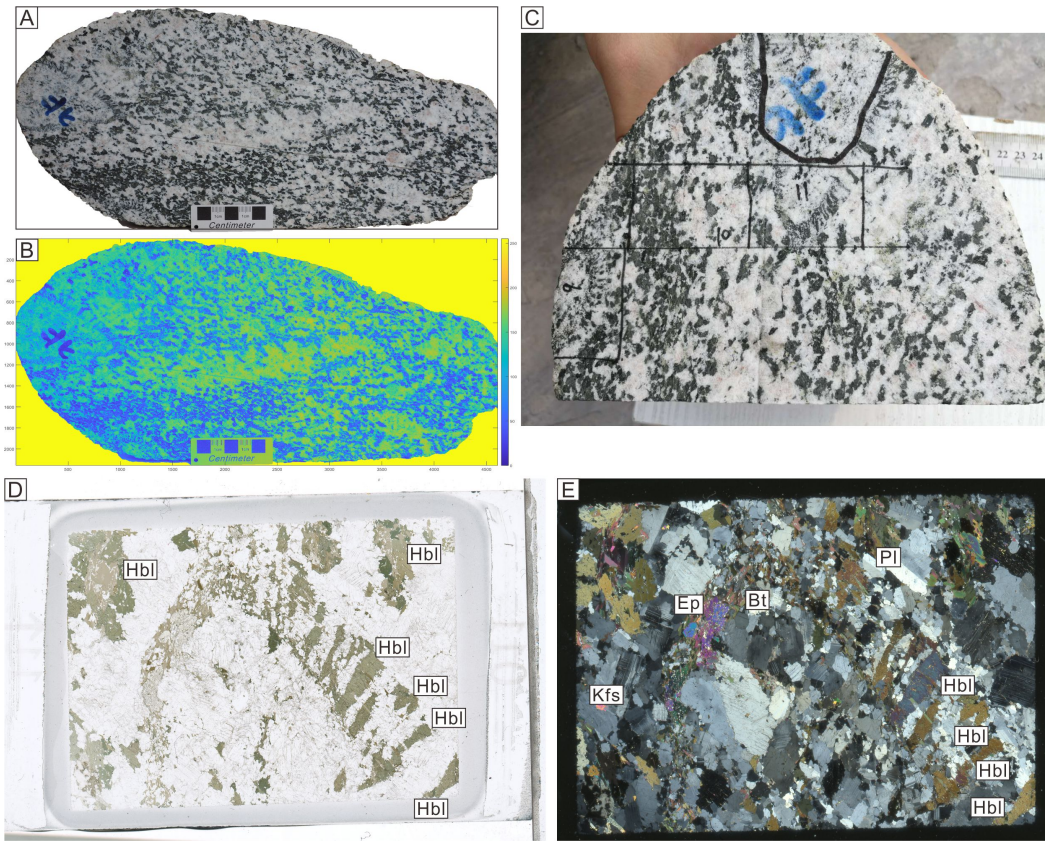

Figure S1. Field photos and photomicrographs of the collected orbicule in the Gangdese belt, southern Tibet. (b) is digitally enhanced from (a). (d) Photomicrograph of part of the orbicule (under plane-polarized light, thin-section 11 in figure c). (e) Photomicrograph of part of the orbicule (under cross-polarized light, thin-section 11 in figure c). The digital enhancement is employed to enhance the texture and mineral distribution patterns.

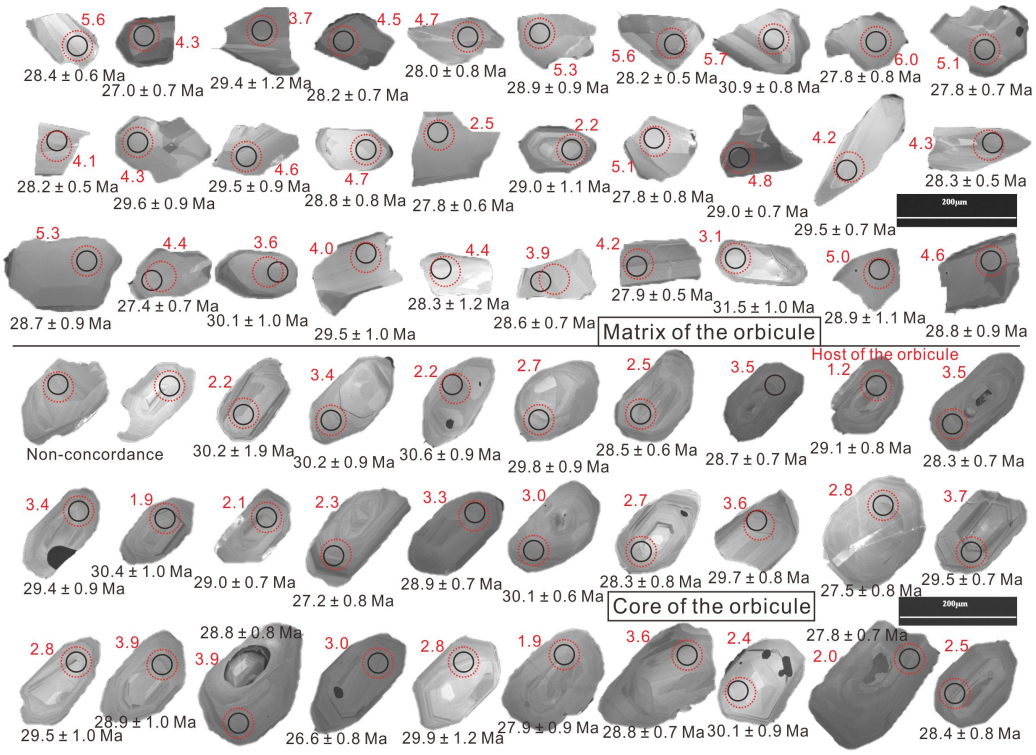

Figure S2. Representative zircon Cathodoluminescence (CL) images and the spots for the zircon U-Pb and Lu-Hf analyses. The black circle denotes the U-Pb dating spot, while the dashed red circle represents the Lu-Hf spots.

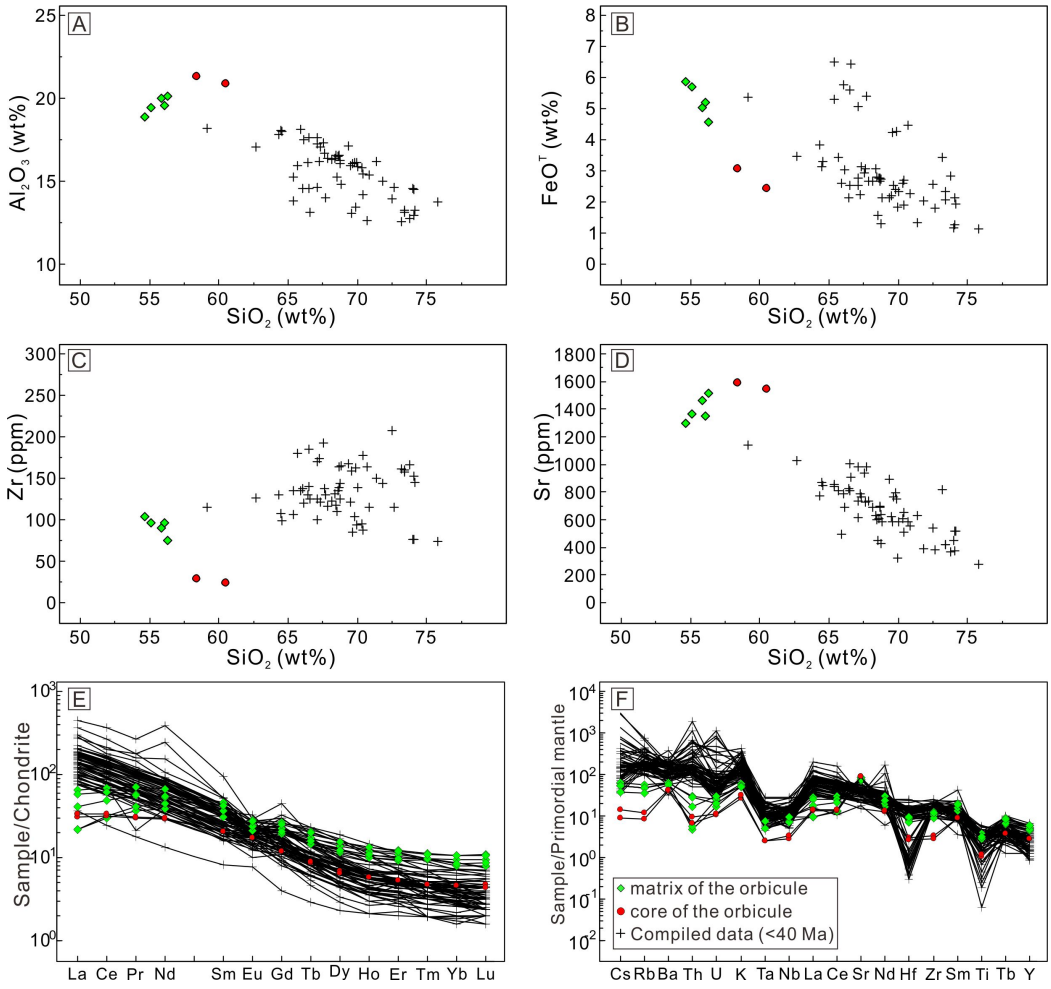

Figure S3. Whole-rock Harker diagrams and trace elemental spider diagrams for the matrix and core of the orbicule. (a-d) Whole-rock Harker diagrams of Al_2O_3 vs. SiO_2, FeO^T vs. SiO_2, Zr vs. SiO_2, and Sr vs. SiO_2. (e) Chondrite-normalized rare earth element diagram. Chondrite standard values are from Sun and McDonough (1989). (f) Primitive mantle-normalized trace elemental spider diagram. Primitive mantle standard values are from Taylor and McLennan (1985). The compiled data for the post-collisional granitic rocks (<40 Ma) are used to identify the provenance of the studied orbicule.

Analytical methods

Micro-XRF scan

A Bruker's M4 Tornado Micro-XRF spectrometer was utilized to perform the XRF analyses, which is an energy dispersive μXRF spectrometer with a motorized X-Y-Z sample stage allowing for different types of measurements including single point analyses, line scan and area mapping. The measurement in this study is carried out with a source voltage of 50 Kv, source current of 600 μA, pixel size of 4 μm and 10 ms per pixel. The XRF scanning was implemented at Key Laboratory of Deep-Earth Dynamics of Ministry of Natural Resources, Institute of Geology, Chinese Academy of Geological Sciences, Beijing 100037, China.

Zircon LA-ICP-MS U-Pb Dating and trace elemental analysis

U-Pb geochronology of zircon was conducted by LA-ICP-MS at Nanjing FocuMS Technology Co. Ltd. An Australian Scientific Instruments RESOlution LR laser-ablation system (Canberra, Australian) and an Agilent Technologies 7700x quadrupole ICP-MS (Hachioji, Tokyo, Japan) were combined for the analyses. The 193 nm ArF excimer laser beam was focused on the zircon surface with a fluence of ~4.5 J/cm^2. Each acquisition incorporated 20 s background (gas blank), followed by spot analyses with a diameter of 33 μm at 6 Hz repetition rate for 40 s. Helium (370 ml/min) was applied as carrier gas to efficiently transport aerosol out of the ablation cell, and was mixed with argon (~1.15 L/min) via a T-connector before entering the ICP torch. Dwell times were set to 20 ms for ^{207}Pb, 15 ms for ^{206}Pb and ^{208}Pb, 10 ms

for ^{232}Th and ^{238}U, and 8 ms for ^{202}Hg, ^{204}Pb and other trace elements.

Zircon 91500 (1062 Ma) was used as external standard to correct instrumental mass discrimination and elemental fractionation during the ablation. GJ-1 (600 Ma) and Plešovice (337 Ma) were treated as quality control for geochronology. Trace elemental abundance of zircon was external calibrated against NIST SRM 610 with Si as an internal standard. Raw data reduction was performed off-line by ICPMSDataCal software (Liu et al., 2010). The analytical results of zircon U-Pb ages and trace elemental concentrations are presented in Table S1 and Table S2 (supporting information), respectively.

Bulk-rock geochemical analysis

Portions of core and matrix were separated by rock saw before analysis. Whole-rock major elements of core and matrix samples were measured using X-ray fluorescence spectrometer (ME-XRF), while trace elements were measured through inductively coupled plasma-mass spectrometry (ICP-MS) and inductively coupled plasma-atomic emission spectrometry (ICP-AES) at ALS Chemex Co. Ltd., Guangzhou, China. Sample powders were fused with lithium metaborate–lithium tetraborate flux, which also includes an oxidizing agent (lithium nitrate), and then poured into a platinum mold to form a disk. XRF analysis of the disk is performed in conjunction with a loss on ignition at 1000°C. The analytical data from both determinations are combined to produce a “total”. Then, the resulting melt is cooled and dissolved in an acid mixture containing nitric, hydrochloric and hydrofluoric

acids. This solution is then analyzed by ICP-MS. A prepared sample is digested with perchloric, nitric, hydrofluoric and hydrochloric acids. The residue is topped up with dilute hydrochloric acid and the resulting solution is analyzed by inductively coupled plasma-atomic emission spectrometry (ICP-AES). The results are corrected for spectral interelement interferences. The analytical results of the whole-rock geochemical analyses are presented in Table S3 (supporting information).

Zircon Lu-Hf analysis

Hafnium isotopic ratios of zircon were conducted by LA-MC-ICP-MS at Nanjing FocuMS Technology Co. Ltd. An Australian Scientific Instruments *RESOlution LR* laser-ablation system (Canberra, Australian) and a Nu Instruments *Nu Plasma II* MC-ICP-MS (Wrexham, Wales, UK) were combined for the analyses. The 193 nm ArF excimer laser, homogenized by a set of beam delivery systems, was focused on the zircon surface with fluence of 4.5J/cm^2. Each acquisition incorporated 20 s background (gas blank), followed by spot analyses with a diameter of 50 um at 9 Hz repetition rate for 40 s. Helium (370 ml/min) was applied as carrier gas to efficiently transport aerosol out of the ablation cell, and was mixed with argon (~0.97 L/min) via a T-connector before entering the ICP torch. Integration time of *Nu Plasma II* was set to 0.3 s (equating to 133 cycles during the 40 s). Standard zircons (including GJ-1, 91500, Plešovice, Mud Tank, Penglai) were analyzed for quality control after every fifteen samples in the present study (Black and Gulson, 1978; Jackson et al., 2004; Wu et al., 2006; Sláma et al., 2008; Li et al., 2010). The zircon Lu-Hf isotopic

compositions are listed in Table S4 (supporting information).

Bulk rock Sr-Nd isotopic analysis

High precision isotopic (Sr and Nd) measurements were carried out at Nanjing FocuMS Technology Co. Ltd. Rock powders were decomposed by high-pressure PTFE bombs. Strontium, Nd, and Pb were all purified from the same digestion solution by two step column chemistry: The first exchange column combined with BioRad AG50W×8 and Sr Spec resin was used to separate Sr and REE from the sample matrix. Neodymium was separated from the other REE on the second column with Ln Spec-coated teflon powder. Hafnium was purified with another Ln Spec resin.

The Sr- and Nd-bearing elutions were dried down and re-dissolved in 1.0 ml 2wt% HNO_3. Small aliquots of each were analyzed using Agilent Technologies 7700x quadrupole ICP-MS (Hachioji, Tokyo, Japan) to determine the exact contents of Sr and Nd available. Diluted solution (50 ppb Sr, 50 ppb Nd doping with 10 ppb Tl) were introduced into Nu Instruments Nu Plasma II MC-ICP-MS (Wrexham, Wales, UK) with a Teledyne Cetac Technologies Aridus II desolvating nebulizer system (Omaha, Nebraska, USA).

Raw data of isotopic ratios were corrected for mass fractionation by normalizing to $^{86}Sr/^{88}Sr = 0.1194$ for Sr and $^{146}Nd/^{144}Nd = 0.7219$ for Nd with exponential law. International isotopic standards (NIST SRM 987 for Sr, JNdi-1 for Nd) were periodically analyzed to correct instrumental drift. Geochemical reference materials of USGS BCR-2, BHVO-2, AVG-2 and RGM-2 were treated as quality control (Weis et

al., 2006). The analytical results of whole-rock Sr-Nd isotopes are listed in Table S5 (supporting information).

Electron Microprobe Analysis

Based on detailed petrographic observations, representative amphiboles from thin sections were selected for electron microprobe analyses (EMPA). Mineral chemical compositions were determined using a JEOL JXA-8100 electron microprobe (EMP) with a ≤5 μm probe beam diameter, counting time of 10 s for peak and 5 s for background under a 15.0 kV accelerating voltage and a 20 nA beam current, at the Institute of Geology, Chinese Academy of Geological Sciences, Beijing 100037, China. Natural hornblende mineral of SPI company was used for standardization, and ZAF corrections were carried out. The hornblende EMPA analytical results are listed in Table S6 (supporting information).

References cited:

Black, L.P., Gulson, B.L., 1978. The age of the Mud Tank carbonatite, Strangways Range, Northern Territory: BMR. Journal of Australian Geology and Geophysics 3, 227–232.

Jackson, S.E., Pearson, N.J., Griffin, W.L., 2004. The application of laser ablation microprobe-inductively coupled plasma–mass spectrometry (LAM–ICP–MS) to in situ U–Pb zircon geochronology. Chemical Geology 211, 47–69.

Li, X.H., Long, W.G., Li, Q.L., Liu, Y., Zheng, Y.F., Yang, Y.H., Chamberlain, K.R., Wan, D.F., Guo, C.H., Wang, X.C., Tao, H., 2010. Penglai zircon megacrysts: a potential new working reference material for microbeam determination of Hf-O

isotopes and U-Pb ages. Geostandards and Geoanalytical Research 34, 117–134.

Liu, Y.S., Hu, Z.C., Zong, K.Q., Gao, C.G., Gao, S., Xu, J., Chen, H.L., 2010. Reappraisement and refinement of zircon U-Pb isotope and trace element analyses by LA-ICP-MS. Chinese Science Bulletin 55, 1535–1546.

Sláma, J., Košler, J., Condon, D.J., Crowley, J.L., Gerdes, A., Hanchar, J.M., Horstwood, M.S.A., Morris, G.A., Nasdala, L., Norberg, N., Schaltegger, U., Schoene, B., Tubrett, M.N., Whitehouse, M.J., 2008. Plešovice zircon — A new natural reference material for U–Pb and Hf isotopic microanalysis. Chemical Geology 249, 1–35.

Weis, D., Kieffer, B., Maerschalk, C., Barling, J., de Jong, J., Williams, G.A., Hanano, D., Pretorius, W., Mattielli, N., Scoates, J.S., Goolaerts, A., Friedman, R.M., Mahoney, J.B., 2006. High-precision isotopic characterization of USGS reference materials by TIMS and MC-ICP-MS. Geochemistry, Geophysics, Geosystems 7, Q08006.

Wu, F.Y., Yang, Y.H., Xie, L.W., Yang, J.H., Xu, P., 2006. Hf isotopic compositions of the standard zircons and baddeleyites used in U-Pb geochronology. Chemical Geology 234, 105–126.